

EFFECT OF GEOMETRY ON STRESS IN PILE
HEAD OF RC SHEET PILE UNDER VERTICAL
IMPACT LOAD

LIM TEIK JIN

SCHOOL OF CIVIL ENGINEERING
UNIVERSITI SAINS MALAYSIA
2022

EFFECT OF GEOMETRY ON STRESS IN PILE HEAD OF RC
SHEET PILE UNDER VERTICAL IMPACT LOAD

By

LIM TEIK JIN

This dissertation is submitted to
UNIVERSITI SAINS MALAYSIA
As partial fulfilment of requirement for the degree of

**BACHELOR OF ENGINEERING (HONS.)
(CIVIL ENGINEERING)**

School of Civil Engineering,
Universiti Sains Malaysia

JULY 2022



**SCHOOL OF CIVIL ENGINEERING
ACADEMIC SESSION 2015/2016**

**FINAL YEAR PROJECT EAA492/6
DISSERTATION ENDORSEMENT FORM**

Title: Effect of Geometry on Stress in Pile Head of RC Sheet Pile
under Vertical Impact Load

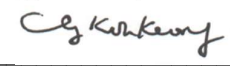
Name of Student: Lim Teik Jin

I hereby declare that all corrections and comments made by the
supervisor(s) and examiner have been taken into consideration and
rectified accordingly.

Signature:



Approved by:




(Signature of Supervisor)

Date : 12 August 2022

Name of Supervisor :
Professor Ir. Dr. Choong Kok Keong

Date : 12 August 2022

Approved by: 

Dr. Mustafasanie M. Yussof
School of Civil Engineering
Universiti Sains Malaysia

(Signature of Examiner)

Name of Examiner :
Dr. Mustafasanie M. Yussof

Date : 12 August 2022

ACKNOWLEDGEMENT

First and foremost, I would like to thank the School of Civil Engineering for providing me an opportunity to do this research for my final year project. The School of Civil Engineering had provided the right academic research platform that was critical to the success of academic researchers. Basically, this research was like a “sneak preview” that exposed several challenges impacting the research work and its progress which would be faced by the academics.

I would like to express my very great appreciation to my supervisor, Professor Ir. Dr. Choong Kok Keong for his invaluable guidance and continuous support throughout the course of this research. He was available whenever I needed to exchange about my idea or any feedback. Had it not been for his advice and assistance in keeping my progress on schedule, this research would not have been possible.

I would also like to extend my heartfelt thanks to Dr. Ong Chong Yong who generously provided his knowledge and expertise. Despite his exceptional busyness, he still patiently lent me a helping hand by guiding and keeping me on the right track. His generosity in spending his time in this research has been very much appreciated.

My appreciation also to Ir. Tan Geem Eng for his valuable and constructive suggestions during the planning and development of this research. The support and information on sheet piling provided by him via mail or through telephone conversations were extremely valuable. Advice given by him had been a great help in this research.

I would also like to show my deep gratitude towards my parents. Their belief in me had kept my spirits and motivation high in accomplishing this research work. Their support and encouragement were important throughout my research.

Lastly, I would like to gratefully acknowledge and thank all the people who helped me. My apologies if I have forgotten to name anybody who helped me with this thesis.

ABSTRAK

Pemanduan impak adalah salah satu sistem pemanduan yang menggunakan siri pukulan tukul untuk memacu cerucuk kepingan ke dalam tanah. Terdapat kejadian yang dilaporkan di mana kepala cerucuk rosak akibat tindakan tukul hentaman. Kegagalan kepala cerucuk menyebabkan kesukaran memandu cerucuk. Dalam industri, kepala cerucuk direka bentuk melalui kaedah percubaan dan kesilapan untuk mengurangkan kerosakan. Kajian sistematik dengan mengambil kira parameter kepala cerucuk yang berbeza perlu dijalankan untuk mengkaji kesan parameter ke atas agihan tegasan dalam kepala cerucuk. Ini adalah untuk mencapai reka bentuk kepala cerucuk yang terbaik dan menjimatkan dalam meminimumkan kerosakan. Perisian LUSAS digunakan untuk simulasi cerucuk kepingan RC dengan beban hentaman menegak bertindak di atasnya. Analisis pertama adalah untuk menentukan beban impak maksimum daripada impak ram tukul yang sesuai digunakan berdasarkan pendekatan yang berbeza. Pendekatan teori gelombang tegasan dan persamaan gerakan memberikan magnitud beban hentaman maksimum yang lebih munasabah berbanding dengan faktor penguatan dinamik. Analisis kedua adalah untuk menentukan kesan nisbah kurungan ke atas taburan tegasan di sepanjang cerucuk kepingan RC. Keputusan menunjukkan bahawa kesan ke atas trend taburan tekanan adalah kecil. Analisis ketiga adalah untuk mengkaji kesan tiga parameter geometri ke atas tegasan dalam kepala cerucuk kepingan RC di bawah beban hentaman menegak. Keputusan menunjukkan bahawa tiada kesan geometri terhadap tegasan dalam kepala cerucuk untuk julat parameter kepala cerucuk yang dipertimbangkan dalam kajian ini.

ABSTRACT

Impact driving is one of the driving systems that applies a series of hammer strikes to drive the sheet pile into the earth. There have been instances reported where pile head is damaged due to the action of impact hammer. The pile head failure causes the difficulty in pile driving. In industry, the pile head is designed through trial-and-error method to reduce the damage. A systematic study with the consideration of different parameters of pile head should be carried out to study the stress distribution within pile head. This is to achieve the best and economical design of pile head in minimizing the damage. LUSAS software is used to simulate the RC sheet pile with the vertical impact load acting on its top. The first analysis is to justify the maximum impact load from the impact of hammer ram based on different approaches. The approaches of stress wave theory and the equation of motion provide a more reasonable magnitude of maximum impact load compared to the dynamic amplification factor. The second analysis is to determine the effect of confinement ratio on stress distribution along the RC sheet pile. The result shows that the effect on the trend of stress distribution is small. The third analysis is to study the effect of geometry on stress in pile head of RC sheet pile under vertical impact load. The result shows that there is no effect of geometry on stress in pile head for the range of pile head parameters considered in this study.

TABLE OF CONTENTS

ACKNOWLEDGEMENT	II
ABSTRAK.....	IV
ABSTRACT	ERROR! BOOKMARK NOT DEFINED.
TABLE OF CONTENTS.....	VI
LIST OF FIGURES.....	X
LIST OF TABLES.....	XIII
LIST OF SYMBOLS	XIV
CHAPTER 1 INTRODUCTION.....	1
1.1. Types of Sheet Pile	1
1.1.1. Wooden Sheet Pile.....	1
1.1.2. Concrete Sheet Pile.....	2
1.1.3. Steel Sheet Pile.....	3
1.2. Interlock Joints	4
1.3. Types of Sheet Piles Walls.....	5
1.3.1. Cantilever Sheet Pile.....	5
1.3.2. Anchored Sheet Pile	6
1.4. Uses of Sheet Piling.....	7
1.4.1. Temporary Applications	7
1.4.2. Permanent Applications.....	7
1.5. Construction Procedures of Sheet Piles.....	8
1.6. Types of Driving Systems.....	10
1.6.1. Impact Driving	10
1.6.2. Vibratory Driving	11
1.7. Background	13
1.8. Problem Statement.....	14
1.9. Objectives.....	16
1.10. Scope of Study.....	17
1.11. Dissertation Outline	17
CHAPTER 2 LITERATURE REVIEW.....	19

2.1.	Introduction	19
2.2.	Stress-Strain Model for Unconfined and Confined Concrete	20
2.2.1.	Concrete in Compression	20
2.2.2.	Concrete in Tension	23
2.3.	Mechanical Properties of Wood	25
2.3.1.	Orthotropic Nature of Wood	25
2.3.2.	Elastic Properties	26
2.4.	Response to Simple Forcing Functions	30
2.4.1.	Suddenly Applied Load with Constant Magnitude and Infinite Duration	30
2.4.2.	Suddenly Applied Load with Constant Magnitude and Finite Duration	32
2.4.3.	Other Simple Loading Cases	34
2.5.	Stress Wave Propagation	36
2.5.1.	Generation of Stress Wave when Ram Impacts the Concrete Pile Head	36
2.5.2.	Reflection of Stress Wave	40
2.6.	Equation of Motion	42
2.6.1.	Pile-Driving Equation	43
2.7.	Impact of Driving Sheet Pile and Franki NG Pile on Weir Construction.....	47
2.7.1.	Franki Piling	49
2.7.2.	Dynamic Measurements and Excitation During Franki NG Piling	51
2.7.3.	Dynamic Measurements and Excitation During Sheet Pile Wall Driving	53
2.8.	Numerical Modelling of Continuous Impact Pile Driving	54
2.8.1.	Effect of Pile Behavior	54
2.8.2.	Comparisons with Previous Numerical Studies	56
2.8.3.	Pile Penetration Process and Propagated Wave Fronts	60
2.9.	Summary	62
CHAPTER 3 METHODOLOGY.....		63
3.1.	Introduction	63
3.2.	Modelling of RC Sheet Pile	64
3.2.1.	Stress Concentration due to Abrupt Change in Form	65
3.2.2.	Geometry of RC Sheet Pile	66
3.2.3.	Material Properties of RC Sheet Pile	69
3.3.	Modelling of Cushion	73

3.3.1.	Geometry of Pile Cushion.....	73
3.3.2.	Material Properties of Pile Cushion.....	74
3.4.	Support Condition.....	77
3.5.	Maximum Impact Loading.....	79
3.5.1.	Approach based on Dynamic Amplification Factor	80
3.5.2.	Approach based on Stress Wave Theory	81
3.5.3.	Approach based on Equation of Motion	83
3.5.4.	Summary of Different Approaches.....	86
3.6.	Convergence Test	87
CHAPTER 4 RESULTS AND DISCUSSION		89
4.1.	Maximum Impact Load from the Impact of Hammer Ram	89
4.1.1.	Stress Contour	90
4.1.2.	Result Tabulation and Graphical Representation.....	94
4.1.3.	Evaluation of Concrete Strength	100
4.1.4.	Mechanisms of Concrete Confinement.....	105
4.1.5.	Summary	106
4.2.	Effect of Confinement Ratio on Stress Distribution.....	107
4.2.1.	Stress Contour	107
4.2.2.	Result Tabulation and Graphical Representation.....	108
4.2.3.	Evaluation of Concrete Strength	112
4.2.4.	Differences between Maximum Compressive Stress and Uniaxial Compressive Strength.....	117
4.2.5.	Summary	121
4.3.	Effect of Geometry on Stress Distribution Within the Pile Head	122
4.3.1.	Stress Contour	123
4.3.2.	Result Tabulation and Graphical Representation.....	124
4.3.3.	Evaluation of Stress Distribution Within the Pile Head	131
CHAPTER 5 CONCLUSION AND RECOMMENDATIONS		133
5.1.	Conclusion.....	133
5.2.	Recommendations	134
REFERENCE		135
APPENDIX A		
APPENDIX B		

APPENDIX C

APPENDIX D

APPENDIX E

APPENDIX F

APPENDIX G

LIST OF FIGURES

Figure 1.1: Wooden sheet pile.....	1
Figure 1.2: Concrete sheet pile.....	2
Figure 1.3: Steel sheet pile.....	3
Figure 1.4: Cantilever sheet pile.....	5
Figure 1.5: Anchored sheet pile.....	6
Figure 1.6: Repetition of process.....	8
Figure 1.7: Second sheet pile installation	8
Figure 1.8: First sheet pile installation.....	8
Figure 1.9: Overview of process	8
Figure 1.10: Impact driving.....	10
Figure 1.11: Vibratory driving	11
Figure 1.12: Parts of concrete sheet pile.....	13
Figure 1.13: Failure of pile head	15
Figure 2.1: Stress-strain model for unconfined and confined concrete	20
Figure 2.2: Calibration of fc _u based on experimental data.....	22
Figure 2.3: Three principal axes of wood	25
Figure 2.4: Time histories response for a prestressed concrete pile driven by steam hammer with a firm cap block: (a) axial force; (b) axial displacement in the pile head.....	32
Figure 2.5: Peak response for the suddenly applied load of constant magnitude but finite duration.	33
Figure 2.6: Peak response for a constant load with finite rise time (after Biggs.....	34
Figure 2.7: Peak response to a suddenly applied triangular load block (after Biggs ..	35
Figure 2.8: Peak response to a symmetric ‘saw tooth’ load block (after Biggs.....	35
Figure 2.9: Generation of idealized stress wave when ram strikes the cushion at the concrete pile head	36
Figure 2.10: Reflection of stress wave at point of a long pile.....	40
Figure 2.11: (a) Definition of diagram for pile-driving equations, (b) Equilibrium of ram. (c) Equilibrium at capblock-pile interface, (d) Diagrams for pile force.	43
Figure 2.12: View of the left abutment.....	48
Figure 2.13: Cross section of machine room on the left abutment with locations of vibration measurements points (◆)	48
Figure 2.14: Weir on Odra river in Wróblin (Opole)	48
Figure 2.15: View of the measuring point No. 4 in the weir gallery.....	48
Figure 2.16: Manufacturing process of Franki NG pile.....	49
Figure 2.17: Results of vibration during Franki NG pile driving on Point No. 1	51
Figure 2.18: Results of vibration during Franki NG pile driving on Point No. 4	51
Figure 2.19: Amplitudes of sheet pile driving a) velocity, b) acceleration.....	53
Figure 2.20: Resulted PPV values for rigid and elastic piles by continuous impact pile driving and based on the PPV values of soil particles at the ground surface.....	54
Figure 2.21: Comparison of the required impact for a 10m pile installation considering elastic and rigid behavior for the pile	55
Figure 2.22: Comparison of computed PPV values with previous numerical results and measured values reported by Wiss (1981) for soil particles at the ground surface.	57
Figure 2.23: Computed PPV values due to the continuous impact pile driving against the envelope of PPV represented by Masoumi et al. (2009).....	58

Figure 2.24: Comparison of computed PPV values with previous numerical results for soil particles at a radial distance of 20m from the pile axis when the pile was located at: (a) 2m depth; (b) 5m depth.....	59
Figure 2.25: Pile penetration during two steps: (a) Initial penetration of the pile due to its self-weight before impact pile driving; (b) Final penetration of the pile due to consecutive hammer impacts.....	60
Figure 2.26: Contours of vertical velocity when hammer impact strikes to pile head at a depth of 6.5m and different elapsed times: (a) 25ms; (b) 50ms; (c) 100ms; (d) 150ms.....	61
Figure 3.1: Overview of methodology.....	63
Figure 3.2: Precast sheet pile manufactured by RIVO PRECAST SDN. BHD.....	64
Figure 3.3: Stress concentration due to abrupt change in form.....	65
Figure 3.4: Corrugated sections of (a) pile head and (b) pile body.....	66
Figure 3.5: Geometry of RC sheet pile.....	66
Figure 3.6: Geometry of RC sheet pile for Model A, B, C, D, E, F, G, H and I.....	68
Figure 3.7: Stress-strain relation for confined concrete M40.....	69
Figure 3.8: f_{cu} versus K.....	70
Figure 3.9: Input for the material properties of RC sheet pile with (a) K=1.2, (b) K=1.6 and (c) K=2.....	72
Figure 3.10: Upper components of pile driving.....	73
Figure 3.11: Geometry of pile cushion.....	73
Figure 3.12: Location of pile cushion.....	74
Figure 3.13: Input for the material properties of pile cushion.....	76
Figure 3.14: Support condition of RC sheet pile.....	77
Figure 3.15: Input for the support condition of RC sheet pile.....	78
Figure 3.16: Maximum impact loading exerted on the pile head with the cushion on its top.....	79
Figure 3.17: Input for the loading of (a) $P_{max,1}$ (b) $P_{max,2}$ and (c) $P_{max,3}$	86
Figure 3.18: Mesh convergence.....	87
Figure 3.19: Tetrahedral.....	88
Figure 3.20: Input for the meshing.....	88
Figure 4.1: Types of variables involved to justify the magnitude of maximum impact load.....	89
Figure 4.2: Stress contours on the full geometry of Model D for $P_{max,1}$	90
Figure 4.3: (a) Vertical cross section and (b) Horizontal cross sections.....	91
Figure 4.4: (n) Vertical cross-section contour and (a-m) Horizontal cross-section contours of σ_z on Model D for $P_{max,1}$	93
Figure 4.5: Maximum and minimum stresses for σ_e	96
Figure 4.6: Maximum and minimum stresses for σ_e based on $F_{max,1}$ only.....	96
Figure 4.7: Maximum tensile and compressive stresses for σ_x	96
Figure 4.8: Maximum tensile and compressive stresses for σ_x based on $F_{max,1}$ only.....	97
Figure 4.9: Maximum tensile and compressive stresses for σ_y	97
Figure 4.10: Maximum tensile and compressive stresses for σ_y based on $F_{max,1}$ only.....	97
Figure 4.11: Maximum tensile and compressive stresses for σ_z	98
Figure 4.12: Maximum tensile and compressive stresses for σ_z based on $F_{max,1}$ only.....	98
Figure 4.13: Concrete failure of RC sheet pile.....	106
Figure 4.14: Types of variables involved to study the effect of confinement ratio on stress distribution.....	107
Figure 4.15: Maximum and minimum stresses for σ_e	110
Figure 4.16: Maximum tensile and compressive stresses for σ_x	110

Figure 4.17: Maximum tensile and compressive stresses for σ_y	110
Figure 4.18: Maximum tensile and compressive stresses for σ_z	111
Figure 4.19: Types of variables involved to study the effect of geometry on stress distribution within the pile head	122
Figure 4.20: Horizontal cross sections considered for the nine models	123
Figure 4.21: Maximum tensile (a) and compressive stresses (b) of σ_z for the nine models	129
Figure 4.22: Taper angle	130

LIST OF TABLES

Table 2.1: Default values of the parameters used.....	23
Table 2.2: Elastic ratios for species at approximately 12% moisture content ^a	26
Table 2.3: Strength properties of woods (metric).....	27
Table 2.4: Poisson’s ratios for species at approximately 12% moisture content	29
Table 2.5: Main differences of the model of Rooz and Hamidi (2019) and previous numerical models.....	56
Table 3.1: Length of respective parts of sheet pile.....	67
Table 3.2: Material properties of RC sheet pile	69
Table 3.3: Elastic ratios of pine spruce (Engelmann).....	75
Table 3.4: Mechanical properties of plywood cushion.....	75
Table 3.5: Summary of different approaches	86
Table 4.1: Maximum and minimum stresses for σ_e	94
Table 4.2: Maximum tensile and compressive stresses for σ_x	94
Table 4.3: Maximum tensile and compressive stresses for σ_y	95
Table 4.4: Maximum tensile and compressive stresses for σ_z	95
Table 4.5: Evaluation of concrete strength based on σ_x	100
Table 4.6: Evaluation of concrete strength based on σ_y	101
Table 4.7: Evaluation of concrete strength based on σ_z	102
Table 4.8: Maximum and minimum stresses for σ_e	108
Table 4.9: Maximum tensile and compressive stresses for σ_x	108
Table 4.10: Maximum tensile and compressive stresses for σ_y	109
Table 4.11: Maximum tensile and compressive stresses for σ_z	109
Table 4.12: Evaluation of concrete strength based on σ_x	112
Table 4.13: Evaluation of concrete strength based on σ_y	113
Table 4.14: Evaluation of concrete strength based on σ_z	114
Table 4.15: Differences between maximum compressive σ_x and uniaxial compressive strength.....	117
Table 4.16: Differences between maximum compressive σ_y and uniaxial compressive strength.....	118
Table 4.17: Differences between maximum compressive σ_z and uniaxial compressive strength.....	119
Table 4.18: Maximum tensile and compressive stresses of σ_z for Model A.....	124
Table 4.19: Maximum tensile and compressive stresses of σ_z for Model B.....	125
Table 4.20: Maximum tensile and compressive stresses of σ_z for Model C.....	125
Table 4.21: Maximum tensile and compressive stresses of σ_z for Model D.....	126
Table 4.22: Maximum tensile and compressive stresses of σ_z for Model E	126
Table 4.23: Maximum tensile and compressive stresses of σ_z for Model F	127
Table 4.24: Maximum tensile and compressive stresses of σ_z for Model G.....	127
Table 4.25: Maximum tensile and compressive stresses of σ_z for Model H.....	128
Table 4.26: Maximum tensile and compressive stresses of σ_z for Model I	128

LIST OF SYMBOLS

K	ratio of confinement
ϵ_{cu}	hoop fracture strain
f_{cu}	stress at the hoop fracture strain
x	normalized strain
f'_{cc}	maximum strength of the confined concrete
ϵ_{cc}	strain at the maximum strength of the confined concrete
ϵ_f	final failure strain of the confined concrete
G	modulus of rigidity
E	modulus of elasticity
μ	Poisson's ratio
σ_c^{\max}	maximum compressive stress at the pile head
W	ram weight
h	ram free fall
g	acceleration due to gravity
V	ram impact velocity
A_c	cross-sectional area of the cushion
E_c	elastic modulus of the cushion
t_c	initial uncompressed thickness of the cushion
t	time
k	cushion stiffness
A	cross-sectional area of the pile
γ	unit weight of the pile

CHAPTER 1

INTRODUCTION

1.1. Types of Sheet Pile

Sheet piles are typically thin piles. They are sections of sheet material with interlock edges that are driven into the ground for the purposes of earth retention and excavation support. These piles are used to resist lateral forces due to earth, water or other loads. They are not meant for supporting the vertical load. The common materials used in the manufacture of sheet piles are wood, concrete and steel.

1.1.1. Wooden Sheet Pile

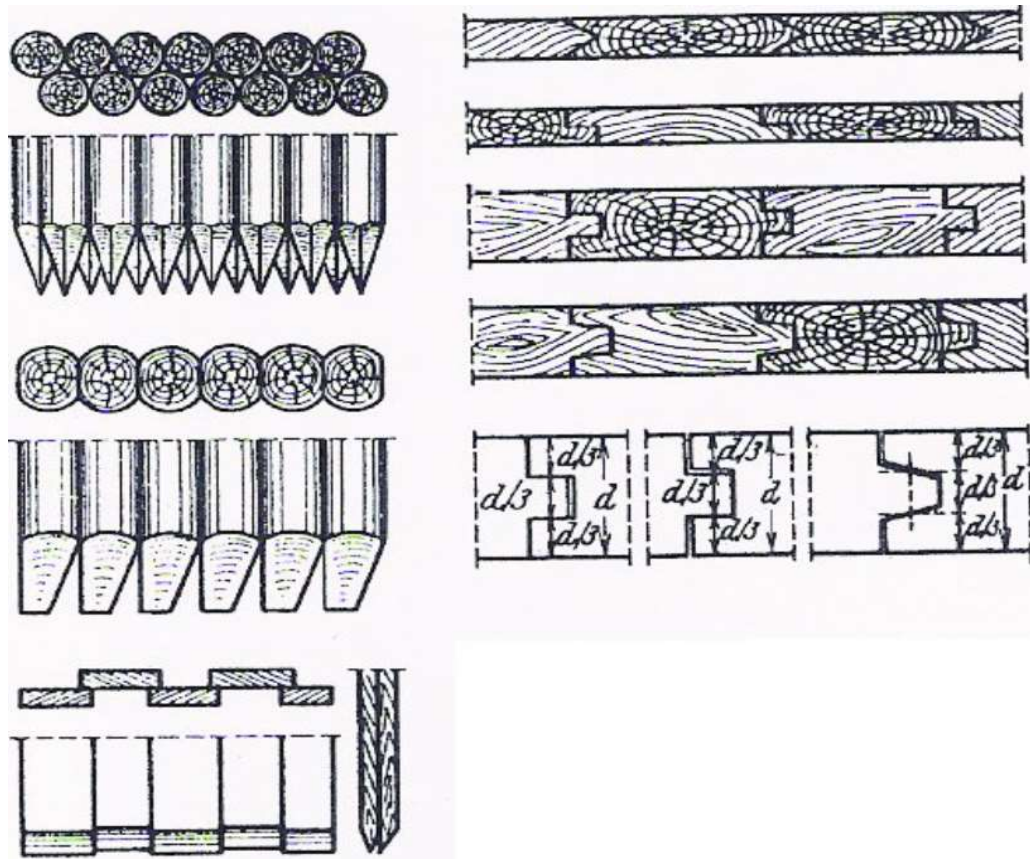


Figure 1.1: Wooden sheet pile

Historically, wooden sheet pile shown in Figure 1.1 is said to be the earliest sort of building material used for temporary light structure to resist light lateral loads and avoid cave-ins. Wood deteriorates with time, particularly when it has been exposed to unfavourable environmental conditions such as dryness and wetness for a long period. It is still applied in some applications nowadays. However, it must be entirely enclosed or coated with chemicals such as aluminium, chrome, or steel plating to prevent rapid deterioration (Eskandari & Kalantari, 2011). It is not suitable to be used for soil that contains stones or rock chips.

1.1.2. Concrete Sheet Pile



Figure 1.2: Concrete sheet pile

Precast concrete sheet pile shown in Figure 1.2 is commonly utilised as retaining wall or bulkhead with the aid of dead man in either salt or fresh water. Although it is aesthetically pleasant, but its driving process is difficult due to its weight. It may cause large disturbance during driving (Eskandari & Kalantari, 2011). Driving resistance to pile increases due to the large volume of soil displacement during driving. It must not be damaged during handling and driving. Proper reinforcement shall be provided within the concrete sheet pile. It is connected to

other by tongue and groove joints. Its toe is typically cut with an oblique face for easy driving and interlocking purposes. Its head is finished off by casting a capping beam at final stage.

1.1.3. Steel Sheet Pile



Figure 1.3: Steel sheet pile

Steel sheet pile shown in Figure 1.3 is widely used in current projects due to its high load resistance, long service life, high driving stress resistance, lightweight, reusability, ease of transporting, ease of driving in various types of soil layers and the necessity for a limited construction area. It is employed in both temporary and permanent structures which include soil consolidation, breakwaters and harbour projects. It can be utilised as watertight barrier due to its better water tightness (steel is an impermeable material), minimal deformation at joints and ease of elongation by welding (Eskandari & Kalantari, 2011). Since steel is prone to corrosion, its durability can be improved with the aid of corrosion protection measures such as coating and cathodic protection. Availability of different cross-section steel sheet piles are depending on their application, safety, and cost. Sections of steel sheet piles are linked together by interlock joints along with the pile lengths, allowing the sections to be fitted together to form one continuous wall (Byfield & Mawer, 2003).

1.2. Interlock Joints

Joining the interlock joints of the side-by-side sheet pile sections by installation in sequence constructs a full sheet pile wall. Since the pile driving action necessitates a certain degree of motion in the interlocks, the connections between sheet piles are not waterproof. Water seeping through the joints may happen. Interlock joints play a vital role during the driving process despite the non-watertight joints between sheet piles (Grabe, 2008). The fine particles of soil or dirt accumulate in the interlock joints over period, producing an action of "self-sealing". The "self-sealing" action of steel sheet pile is augmented by corrosion. Based on the section 8.1.20.3 of EAU 2004 (R 117), the installation of environmentally compatible synthetic sealants can aid this natural sealing process for the walls standing in water.

When sheet piles are driven with an impact hammer, the seals are less stressed due to the movement restriction in one direction only. However, vibratory driving the sheet piles induces large load on the seals due to the generated friction and the associated increase of temperature. Improper interlocking between a sheet pile and its neighbour may cause declutching. Interlock damage cannot be totally avoided, regardless of how careful driving. It is advised to have declutching check to improve the reliability of the sheet pile wall.

1.3. Types of Sheet Piles Walls

Sheet piles can be interconnected and driven into the ground to form a continuous sheet pile wall. The wall is also called as bank heads. The common types of sheet piles walls are cantilever sheet pile and anchored sheet pile.

1.3.1. Cantilever Sheet Pile

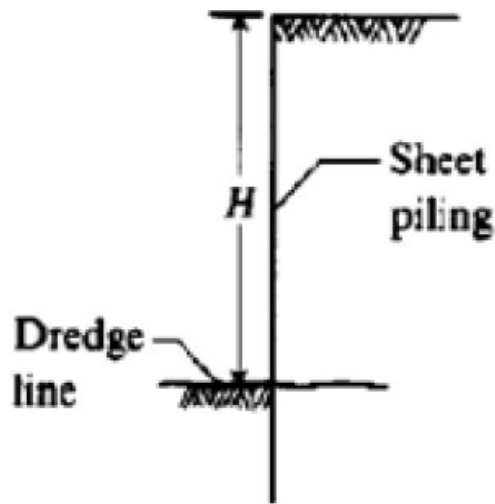


Figure 1.4: Cantilever sheet pile

For free cantilever sheet pile, it is subjected to a concentrated horizontal load at its top with no backfill above the dredge level. For cantilever sheet pile shown in Figure 1.4, it is backfilled at a higher level on one side. The cantilever sheet pile is commonly utilised for excavations up to 6m above the dredge line. Both types of cantilever sheet piles derive their stability from the higher passive resistance of soil under the dredge level into which they are driven. In practise, it is utilised as retaining structure for preserving permanent or temporary excavations in many project fields involved with geotechnical operations (Eskandari & Kalantari, 2011). In addition, it functions as temporary protection in foundation constructions (Babu & Basha, 2008).

1.3.2. Anchored Sheet Pile

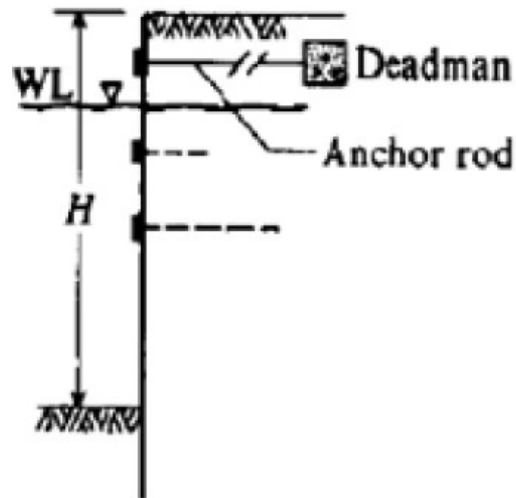


Figure 1.5: Anchored sheet pile

Anchored sheet pile shown in Figure 1.5 is considered as a cost-effective type of sheet pile for the depth not exceeding six meters. Anchor installation necessitates just a minor excavation for equipment access. Anchoring the sheet pile at the top of its bracing causes shallower penetration depth and less moment induced to the sheet pile. Proper installed anchor wall has less horizontal deflection than braced wall, thereby providing a better control of back-slope subsidence. The anchor is stressed to a small nominal load and temporarily locked-off to essentially reduce slack from the anchors (ground anchors and anchored systems). Therefore, anchored wall operates in close proximity to prestressed concrete structure. However, the vertical sediment of sheet wall may possibly occur due to the vertical component of anchor forces (Eskandari & Kalantari, 2011). Subsidence of the anchor system may also happen because of the caving of anchor hole prior to grouting and flow of non-cohesive material into the excavation via wall hole created for anchor placement.

1.4. Uses of Sheet Piling

Uses of sheet piling can be categorized as permanent and temporary applications (ESC, n.d.). Temporary sheet piles are installed temporarily. After completion of construction, the sheet piles will be extracted for reuse. Permanent sheet piles are installed permanently.

1.4.1. Temporary Applications

1. For the construction that may be done at a limited space, temporary wall is built to avoid cave-in. Workers in the surrounding region are protected by the temporary wall.
2. Temporary sheet piles are utilised in temporary works to perform the deep excavation and facilitate the construction below ground and water level.
3. To support the excavation for the constructions of basement, parking structure, foundation and pump house.

1.4.2. Permanent Applications

1. For a home environment, permanent walls are used to provide better durability and stability to the interior walls (especially basement walls).
2. To protect foundations from the damage of water ingress.
3. To serve as retaining walls for structures such as basements, bridge abutments, quay walls, underground storage tanks and underground car parks.

4. To serve as river embankment (prevent floods to area or structure closes to shoreline).
5. To serve as earth retaining.
6. To serve as cofferdams, seawalls and bulkheads.

1.5. Construction Procedures of Sheet Piles

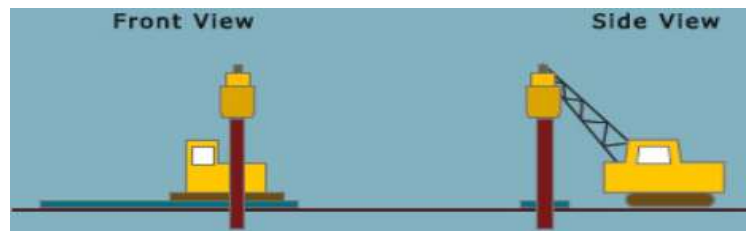


Figure 1.6: First sheet pile installation



Figure 1.7: Second sheet pile installation

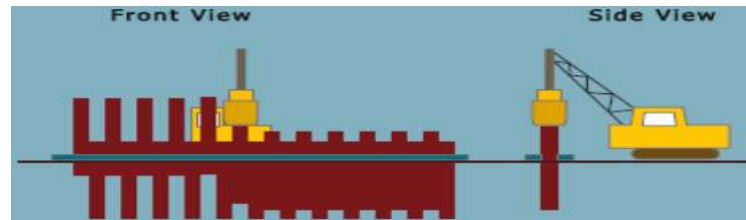


Figure 1.8: Repetition of process

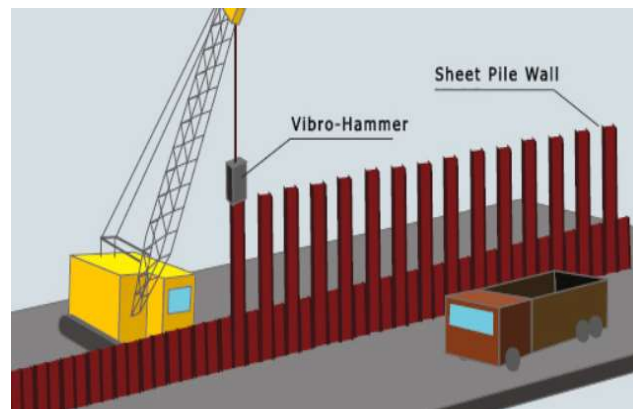


Figure 1.9: Overview of process

Sheet piles are typically installed with vibratory hammer. Impact hammer will be used for driving pile into a very dense or hard soil. If the required pile penetration by vibratory hammer is unattained and further penetration is not allowed, vibratory driving mode will be switched to impact driving mode to forcibly drive the pile into the soil.

1. Sheet piles should be thoroughly examined for the straightness, fractures, and integrity of the interlocking components prior to installation. A sequence of sheet pile sections is laid out to ensure the sheet piles will interlock properly.
2. The sheet piles are driven individually to the certain required depth (Figure 1.6). The first sheet pile is driven to be interlocked with the second sheet pile (Figure 1.7).
3. The driving process should be closely supervised. The pile driving should be stopped promptly if the pile penetration stops, before proceeding to the next pile along. Several adjacent piles may be unable to further penetrate to achieve the design depth in some instances. At this stage, an attempt should be done to eliminate the impediment, either by partial excavation or applying a water jet. There is a certain number of ‘under-driven’ sheet piles which are acceptable. However, it varies and depends on the specific design requirements.
4. Step 2 is repeated until the required wall perimeter is completed (Figure 1.8).

A minimum of 0.30 m pile head should be extended into the pile cap. Before pouring the cap, any damaged portions of the pile head should be trimmed and removed down to undamaged part. For piles that are attached to the cap by embedded bars or strands, a minimum of 0.15 m pile head should be extended into the pile cap (FHWA, 2016).

1.6. Types of Driving Systems

There are two types of driving systems that are applicable to the sheet pile: Impact driving and vibratory driving.

1.6.1. Impact Driving

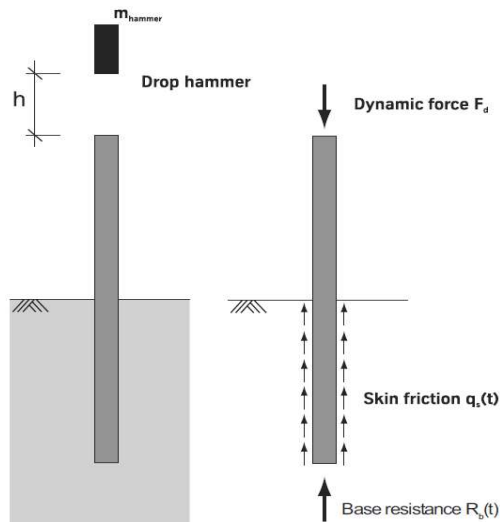


Figure 1.10: Impact driving

Impact driving shown in Figure 1.10 is a method of applying a series of hammer strikes to drive the sheet pile into the earth. A cushion positioned between the sheet pile and hammer is normally a wooden driving cap. The systems of impact driving can be slow-action system or fast-action system. For the condition where pile is driven into the cohesive soil, the slow-action system such as diesel hammer and

drop hammer is mainly applied to allow the dissipation of pore water pressure due to the subsequent individual impacts. The drop hammer has a mass that is required to be mechanically uplifted and released from a certain height. Modern drop hammer can be hydraulically operated. A range of 24 - 32 strikes per minute can be set as the number of strikes needed (Grabe, 2008). The explosion of air mixture or diesel fuel in a cylinder governs the drop height of the diesel hammer. There are two drop motions of mass (depends on the hammer type): [1] the mass can be free fall onto the driving cap, or [2] the mass is slowed down by an air buffer on its upward motion and then accelerated by a spring on its downward motion. The latter method allows higher strikes per minute compared to the non-accelerated hammer. For the fast-action system, the compressed air is applied to drive the system. Its mass accelerates as it drops from a certain height. Although the driving weight of fast-action hammer is correspondingly lighter, a range of 100 – 400 strikes per minute can be set as the number of strikes needed.

1.6.2. Vibratory Driving

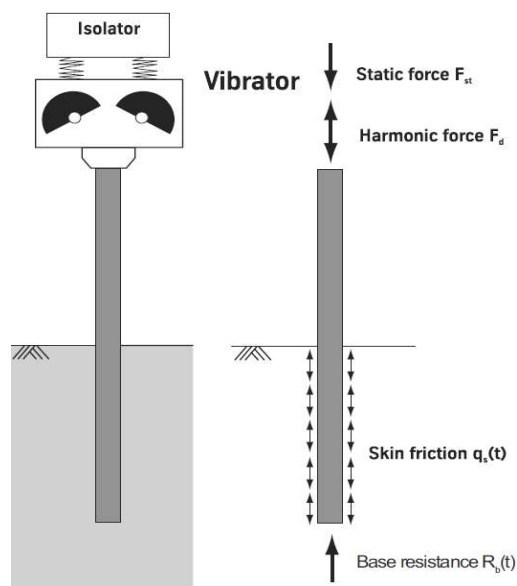


Figure 1.11: Vibratory driving

Vibratory driving shown in Figure 1.11 is a vibrating method that can harmonically excite the sheet pile. It can cause the soil redistribution, thereby reducing the toe resistance and the friction between the sheet pile and the soil (skin resistance). It also can cause the occurrence of local soil liquefaction at the boundary layer between the soil and the sheet pile, thereby decreasing the driving resistance. Besides driving the sheet piles, the vibratory driving also can be used for extracting piles. The eccentric weights of vibrator generate the harmonic excitation. During the rotation of eccentric weights, the transmission of oscillations to the pile-driving plant can be prevented by the isolator. The self-weight of vibrator loads the sheet pile with a static force. The equation of maximum centrifugal force, F_d is $F_d = m_u r_u \Omega^2$, where Ω is the exciter frequency, m_u is the mass of eccentric weights and r_u is the distance of centre of gravity of the eccentric weights to the rotation point. A static moment is defined as the product of m_u and r_u .

The vibrator suspended from a crane or excavator is mounted on the sheet pile head. It is driven hydraulically. For modern vibrator, its static moment and frequency can be adjusted to match the soil properties for optimizing the driving progress. The braking and acceleration of eccentric weights in vibratory driving may allow the occurrence of low frequencies, thereby exciting the natural frequency of the suspended floor (estimated 8–15 Hz) and the building (estimated 1–5 Hz) (Grabe, 2008). Nowadays, vibrator can function at the maximum revolutions per minute (r.p.m.) at first and its rotation of eccentric weights produce a variable imbalance moment from zero to maximum.

1.7. Background

Concrete sheet-piling consists of interlocked concrete sections driven into the ground to form a continuous wall with required perimeter. The two basic categories of concrete sheet piles are cast-in-place concrete sheet piles and precast sheet piles. Cast-in-place concrete sheet piles are sheet piles that are cast at the site in formwork. Since they are made in place to correct length (dimension), they generally need no storage space and special handling. Precast sheet piles are sheet piles that are prepared, cast and cured off-site. In general, concrete sheet piles are specially designed to be driven into soils and provide structural support or barriers for water and soils.

Vibratory driving is typically used to drive the concrete sheet piles into the ground. If the required pile penetration by vibratory hammer is unattained and further penetration is not allowed, vibratory driving mode will be switched to impact driving mode to forcibly drive the pile into the soil. Impact hammer is used for driving pile into a very dense or hard soil.

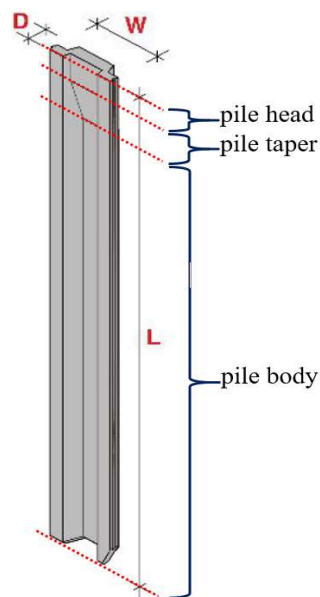


Figure 1.12: Parts of concrete sheet pile

There are three main parts of concrete sheet pile: pile head, pile taper and pile body. Both pile head and pile body have the uniform cross-sectional area throughout their lengths. However, the pile head is much thicker and bulkier than the pile body. The part in between pile head and pile body is pile taper. The cross-sectional area of pile taper is gradually changed throughout its length.

There have been instances reported where pile head is damaged due to the action of impact hammer. The damage of pile head causes the driving forces generated cannot be effectively transferred to the pile body. Since the pile head is the main part that is specially manufactured to resist the high driving stresses, the pile head failure may cause difficulty in pile driving and therefore it leads to inadequate pile length to be embedded into the soil. So, the change in the design of pile head can reduce the possibility of damage. However, it requires information on stress distribution within the pile head under the action of impact hammer.

1.8. Problem Statement

Impact driving is a common method of applying a series of hammer strikes to drive the sheet pile into the earth. For the condition where the required pile penetration by vibratory hammer is unattained and further penetration is not allowed, the vibratory driving mode will be switched to the impact driving mode to forcibly drive the pile into the soil. The drop hammer has a mass that is required to be mechanically uplifted and released from a certain height. A cushion positioned between the sheet pile and hammer is normally used to absorb the initial hammer shock when impact force is transmitted to the pile, thereby minimizing the damage to concrete piles during the installation process.



Figure 1.13: Failure of pile head

Despite of the pile cushion, it has been observed that the concrete pile head starts spalling until its structural strength is affected. The damage of concrete at the pile head is caused by high or irregular compressive stress concentrations during installation (Figure 1.13). The possible causes of this damage are listed as below:

1. Lack of pile cushioning material between the drive head and the concrete pile, resulting in a very high compressive stress on impact of the hammer ram.
2. The top of pile is not square or perpendicular to the longitudinal axis of the pile, resulting in an eccentric hammer blow and high stress concentrations.
3. Improper alignment of the hammer and pile, resulting in an eccentric hammer blow that causes high stress concentrations.
4. Impact on longitudinal reinforcing steel protruding above the pile head, thereby causing high stress concentration.
5. Lack of adequate transverse reinforcement (confinement) at the pile head.
6. The top corners and edges of the pile head are not chamfered, leading the corners or edges to spall.
7. Fatigue failure of the concrete under a series of hammer strikes at a high stress level.

When the pile head is damaged, there is no other parts of concrete sheet pile which are specially designed to resist the impact of the hammer ram. The impact driving might not be able to continue driving the pile into the soil with the required penetration to achieve its stability geotechnically. Pile head is designed through trial-and-error method to reduce the damage in the industry. The issue is how to achieve a best design to minimize damage and at the same time be economical. Therefore, a systematic study with the consideration of different parameters of pile head should be carried out to study the stress distribution within pile head. This may help in better design of pile head geometry.

The finite element method (FEM) model capable of obtaining the stress distribution within pile head under the impact loading can be carried out. The estimation of maximum impact load from the impact of hammer ram is one of the important inputs needed for the FEM model. During impact driving, the RC sheet pile subjected to uniaxial compressive loading is confined by transverse reinforcement. Therefore, the confinement ratio is required to be considered in the FEM model.

1.9. Objectives

The objectives of this study are as follows:

1. To determine the maximum impact load from the impact of hammer ram.
2. To determine the effect of confinement ratio on stress distribution along the RC sheet pile.
3. To study the effect of geometry with different lengths of pile head, pile taper and pile body on stress in pile head of RC sheet pile under vertical impact load.

1.10. Scope of Study

This study focuses on analysing the effect of geometry on stress in pile head of RC sheet pile under vertical impact load. The geometry refers to the different lengths of pile head, pile taper and pile body. It is assumed that the driving condition where the required pile penetration by vibratory hammer is unattained and further penetration is not allowed. Impact hammer is used for driving the sheet pile forcibly into a very dense or hard soil. This hard driving condition causes no or very little movement of sheet pile penetrating into the soil. LUSAS software is used to simulate the RC sheet pile with the vertical impact load acting on its top. The output data of stress components are used to analyse the stress distribution within the pile head.

1.11. Dissertation Outline

In this dissertation, there are five chapters that have been outlined as below:

Chapter 1 consists of the introduction of the thesis. It gives foreword about the aspects of sheet piles and the driving systems. The chapter gives an overview of the thesis including five important elements: background of the study, problem statement, objective of the study and scope of study.

Chapter 2 consists of the literature reviews of the study. It provides the aspects that are required for the generation of input data (pre-processing) for LUSAS software. However, no relevant study on the effect of geometry on stress in pile head of RC sheet pile under vertical impact load has been found.

Chapter 3 deals with the methodology of the study. It elucidates the generation of input data for the model.

Chapter 4 presents the result and discussion of the study. It commences with the results generated from the simulation (display of output data). The results are visualized and analysed.

Chapter 5 concludes the discussion that has been determined throughout the whole study. The finding of research is stated in this chapter. Recommendations are also suggested for further research work.

CHAPTER 2

LITERATURE REVIEW

2.1. Introduction

The literature review consists of eight sections, including the first section as the introduction of this chapter. The second section, Section 2.2. underlines the simplified stress-strain model for the concrete in compression and tension. It is referred to determine the properties of concrete. Section 2.3. underlines the mechanical properties of the wood species. It is referred to determine the properties of wood cushion. Section 2.4. underlines the response to simple forcing functions. It is referred to estimate the dynamic amplification factor (DAF). Section 2.5. underlines the propagation of waves in impact driven piles. It is referred to estimate the maximum compressive stress at the pile head. Section 2.6. underlines the equation of motion for a mass-spring system considering the pile, capblock and ram. It is referred to estimate the maximum impact force generated from the impact driving. Section 2.7. underlines the impact of driving sheet pile and Franki NG Pile on weir construction. It shows the dynamic measurements and excitation during the Franki NG piling and sheet pile wall driving. The last section, Section 2.8. underlines the numerical modelling of continuous impact pile driving. It covers the aspects of the effect of pile behavior, comparisons between previous numerical studies, pile penetration process and propagated wave fronts.

No relevant study on the effect of geometry on stress in pile head of RC sheet pile under vertical impact load has been found.

2.2. Stress-Strain Model for Unconfined and Confined Concrete

Madhu (2009) proposed the stress-strain relations for unconfined and confined concrete to overcome some flaws of existing commonly used models. The proposed stress-strain relations are validated for a whole range of concrete strengths and confining stresses. Comparison of results between those obtained from a computational fiber-element analysis using the proposed stress-strain model and another widely used existing model show good agreement.

2.2.1. Concrete in Compression

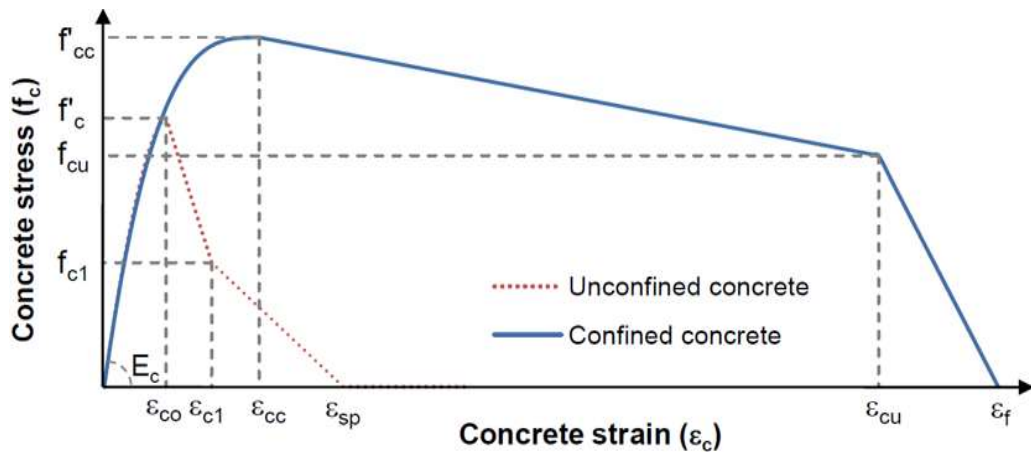


Figure 2.1: Stress-strain model for unconfined and confined concrete

The simplified stress-strain model proposed by Madhu (2009) for the unconfined and confined concrete in compression is shown in Figure 2.1. There are three sets of the coordinates governing the model. The peak compressive strength (ϵ_{co}, f'_c) , at the end of the post-peak part (ϵ_{c1}, f'_{c1}) , and the strain at failure $(\epsilon_{sp}, 0)$ are the primary control coordinates for the unconfined concrete. (ϵ_{cc}, f'_{cc}) , (ϵ_{cu}, f'_{cu}) and $(\epsilon_f, 0)$ are the principal coordinates for the confined concrete. The points of commencement and termination are defined by these coordinates. Based on Figure 2.1, the power curve up until the peak stress and then followed by the bilinear

correlation in the post-peak part. So, three branches are involved in the simplified stress-strain model. The equations of the simplified stress-strain relation:

$$0 \leq x < 1 \quad f_c = Kf'_c(1 - 11 - xl^n) \quad (2.1)$$

$$1 \leq x < x_u \quad f_c = Kf'_c - (f'_c - 12)\left(\frac{x - 1}{x_u - 1}\right) \quad (2.2)$$

$$x_u \leq x < x_f \quad f_c = f_{cu}\left(\frac{x - x_f}{x_u - x_f}\right) \quad (2.3)$$

where,

$$x = \varepsilon_c / \varepsilon_{cc}$$

$$x_u = \varepsilon_{cu} / \varepsilon_{cc} = 5$$

$$x_f = \varepsilon_f / \varepsilon_{cc}$$

K = ratio of confinement

(K = 1 for the unconfined concrete; K > 1 for the confined concrete)

ε_{cu} = hoop fracture strain

f_{cu} = stress at the hoop fracture strain

x = normalized strain

$f'_{cc} = Kf'_c$ = maximum strength of the confined concrete

ε_{cc} = strain at the maximum strength of the confined concrete

$\varepsilon_f = 0.004 + \varepsilon_{cu}$ = final failure strain of the confined concrete

The deficiency of the governing stress-strain relation based on the Mander model (Mander et al., 1989) is lacking the requisite control over the slope of the post-peak part. It is especially true for the concrete with high strength properties (Li et al., 2001). Therefore, the above equations (2.1) – (2.3) are proposed with the ease of algebraic manipulation.

All parameters expressed below are required to be considered in the equations (2.1) – (2.3).

$$\varepsilon_{cc} = \varepsilon_{co}[1 + 5(K - 1)] \quad (2.4)$$

$$\varepsilon_{co} = 0.0015 + \frac{f'_c(\text{MPa})}{70000} \quad (2.5)$$

Concrete modulus $E_c = 5000\sqrt{f'_c(\text{MPa})} \quad (2.6)$

For unconfined concrete $n = \frac{E_c \varepsilon_{co}}{f'_c} \quad (2.7)$

For confined concrete $n = \frac{E_c \varepsilon_{cc}}{f'_{cc}} \quad (2.8)$

$$\varepsilon_{sp} = 0.012 - 0.0001f'_c \quad (2.9)$$

$$f_{cu} = 12 + f'_c(K - 1) \text{ in MPa} \quad (2.10)$$

$$f'_{cc} = Kf'_c \quad (2.11)$$

$$\varepsilon_f = 0.004 + \varepsilon_{cu} \quad (2.12)$$

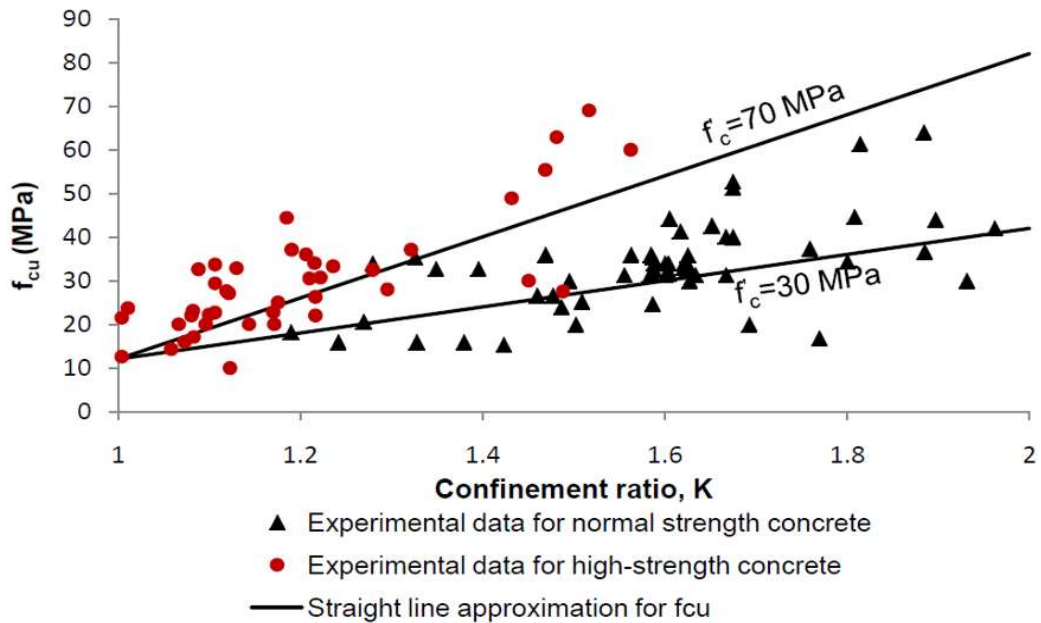


Figure 2.2: Calibration of f_{cu} based on experimental data

Figure 2.2 shows the straight line fit and the dispersion of experimental f_{cu} values. The equation of f_{cu} has been essentially modified to correspond to the original Mander model. It is expressed based on the data from the experimental results of Mander et al. (1989) and Li et al. (2001).

The strain expressed as a function of stress can be obtained by rearranging the above three equations.

$$x = 1 - \left(1 - \frac{f_c}{Kf'_c}\right)^{\frac{1}{n}} \quad (2.13)$$

$$x = 1 + \left(\frac{Kf'_c - f_c}{f'_c - 12}\right)(x_u - 1) \quad (2.14)$$

$$x = x_f + \frac{f_c}{f_{cu}}(x_u - x_f) \quad (2.15)$$

For unconfined concrete where $K=1$, $\varepsilon_{cc} = \varepsilon_{co}$, $\varepsilon_{cu} = \varepsilon_{c1} = 0.0036$, $\varepsilon_f = \varepsilon_{sp}$ and $f_{cu} = f_{c1}$ are considered in all of the above equations.

2.2.2. Concrete in Tension

Table 2.1: Default values of the parameters used

Unconfined (compression)	Confined (compression)	Tension
Peak stress		
f'_c	$f'_{cc} = Kf'_c$	$f'_t = 0.625\sqrt{f'_c(\text{MPa})}$
Peak strain		
$\varepsilon_{co} = 0.0015 + \frac{f'_c(\text{MPa})}{70000}$ ^a	$\varepsilon_{cc} = \varepsilon_{co}[1 + 5(K - 1)]$ ^b	$\varepsilon_{ct} = 0.1\varepsilon_{co}$
Ultimate stress		
$f_{c1} = 12 \text{ MPa}$ ^a	$f_{cu} = 12 + f'_c(K - 1)$ ^c	$f_{t1} = \frac{f'_t}{3}$ ^d

Ultimate strain		
$\varepsilon_{c1} = 0.0036^a$	$\varepsilon_{cu} = 5\varepsilon_{cc}^c$	$\varepsilon_{t1} = \frac{2\varepsilon_u}{9}^d$
Failure strain ^e		
$\varepsilon_{sp} = 0.012 - 0.0001f'_c$ (MPa)	$\varepsilon_f = 0.004 + \varepsilon_{cu}$	$\varepsilon_u = \frac{18G_f(\text{MPa})}{5f'_t h}^d$

- ^a According to predicted stress-strain relation of normal-weight concrete (Collins and Mitchell, 1994).
- ^b Mander et al. (1989).
- ^c According to reevaluation of data from Mander et al. (1989) and Li et al. (2001).
- ^d Rots et al. (1985), where G_f = fracture energy = $h \times$ area under stress-strain softening diagram and h = crack band width.
- ^e Failure stress = 0 for all cases.

The stress-strain model for the confined concrete in tension may be considered using the same approach as that discussed above for the confined concrete in compression. However, new sets of principal control coordinates for the tensile behaviour of concrete require to be defined. The new terms of (ε_{to}, f'_t) , $(\varepsilon_{t1}, f_{t1})$ and $(\varepsilon_u, 0)$ are used to replace the corresponding terms of $(\varepsilon_{cc}, f'_{cc})$, $(\varepsilon_{cu}, f_{cu})$ and $(\varepsilon_f, 0)$ in compression. The approximate values of f'_t , ε_{to} , f_{t1} , ε_{t1} and ε_u are determined as 10% of their corresponding values in compression, or else equations shown in Table 2.1 may be used.